Journal of Thermal Analysis and Calorimetry, Vol. 92 (2008) 3, 893–897

CONTROLLED RATE THERMAL ANALYSIS OF HYDROMAGNESITE

Veronika Vágvölgyi[1], *R. L. Frost*[2*], *M. Hales*[2], *A. Locke*[2], *J. Kristóf*[1] *and Erzsébet Horváth*[3]

[1]Department of Analytical Chemistry, University of Pannonia, 8201 Veszprém, PO Box 158, Hungary
[2]Inorganic Materials Research Program, School of Physical and Chemical Sciences, Queensland University of Technology
2 George Street, GPO Box 2434, Brisbane, Queensland 4001, Australia
[3]Department of Environmental Engineering and Chemical Technology, University of Pannonia, 8201 Veszprém, PO Box 158, Hungary

The reaction of magnesium minerals such as brucite with CO_2 is important in the sequestration of CO_2. The study of the thermal stability of hydromagnesite and diagenetically related compounds is of fundamental importance to this sequestration. The understanding of the thermal stability of magnesium carbonates and the relative metastability of hydrous carbonates including hydromagnesite, artinite, nesquehonite, barringtonite and lansfordite is extremely important to the sequestration process for the removal of atmospheric CO_2. This work makes a comparison of the dynamic and controlled rate thermal analysis of hydromagnesite and nesquehonite. The dynamic thermal analysis of synthetic hydromagnesite proves that dehydration takes place in two steps at 135 and 184°C, dehydroxylation at 412°C and decarbonation at 474°C. Controlled rate thermal analysis shows the first dehydration step is isothermal and the second quasi-isothermal at 108 and 145°C, respectively. In the CRTA experiment both water and carbon dioxide are evolved in an isothermal decomposition at 376°C.

CRTA technology offers better resolution and a more detailed interpretation of the decomposition processes of magnesium carbonates such as nesquehonite via approaching equilibrium conditions of decomposition through the elimination of the slow transfer of heat to the sample as a controlling parameter on the process of decomposition. Constant-rate decomposition processes of non-isothermal nature reveal partial nesquehonite structure.

Keywords: *CRTA, hydromagnesite, lansfordite, magnesite, nesquehonite, thermal analysis, thermogravimetry*

Introduction

The thermoanalytical studies of basic hydroxy-carbonates such as magnesite are not new, even though the first reported studies were in 1910 [1–9]. A similar lack of recent studies is true of minerals such as hydroxyzincite and hydromagnesite [1–3, 5, 10–14]. There is a need to undertake a systematic study using the latest technology of carbonate and hydroxyl-carbonate minerals using thermo-analytical techniques including dynamic and controlled rate thermal analysis. Very few thermoanalytical [9, 15] and spectroscopic studies of the hydroxy carbonates have been forthcoming and what studies that are available are not new. Few Raman studies of any note are available [16, 17]. To the best of the authors knowledge few recent thermoanalytical studies of hydromagnesite have been undertaken [1, 4], although differential thermal analysis of some related minerals has been published [12]. The decomposition of aurichalcite, hydrozincite and hydromagnesite may result in the formation of metal oxides or a mixture of metal oxides such as CuO and ZnO. Both these oxides may function as catalysts and photo-catalysts. The thermal activation of aurichalcite results in the formation of the oxide mixture, mixed at the molecular level and not at the particle level.

Hydromagnesite $Mg_5[(CO_3)_4(OH)_2]\cdot 4H_2O$ is a low temperature hydrothermally formed mineral [18–20]. Under natural conditions hydromagnesite may form in evaporites depending on the availability of the Mg^{2+} ions in solution in relation to the availability of other cations such as Ca^{2+} [18]. The highly hydrated nature of the Mg^{2+} ion prevents the formation of anhydrous $MgCO_3$ phases [19]. Additionally hydromagnesite can form as efflorescences on existing carbonate rocks, man-made bricks and mortars, serpentinites, volcanic breccias and even meteorites [21–25]. The conditions of formation are claimed to be independent of the carbon dioxide partial pressure [18]. The mineral is also formed in caves from water that has seeped through Mg-rich rocks [25]. The formation of carbonates such as hydromagnesite may be a key to the sequesteration of carbon dioxide [26, 27] i.e. the removal of green house gases from the atmosphere.

Recently thermogravimetric analysis has been applied to some complex mineral systems [28–41] and it is considered that TG-MS analysis may also be applicable to many carbonate minerals [32, 42–46]. Raman spectroscopy has proven very useful for the study of minerals [47–49]. Indeed Raman spectroscopy has proven most useful for the study of diagenetically related minerals as often occurs with carbonate

---

[*] Author for correspondence: r.frost@qut.edu.au

1388–6150/$20.00

Akadémiai Kiadó, Budapest, Hungary
Springer, Dordrecht, The Netherlands

minerals [50–54]. Some previous studies have been undertaken by the authors using Raman spectroscopy to study complex secondary minerals formed by crystallisation from concentrated carbonate solutions [55].

The study of the carbonates of magnesium is of extreme importance in the development of technology for the removal of green house gases. Magnesium minerals such as brucite, periclase and hydrotalcites have the potential for the sesquestration of carbon dioxide. The formation and reaction pathways of hydroxy and hydrous carbonates of magnesium is essential for the understanding of this sequestration. The hydration-carbonation or hydration-and-carbonation reaction path in the $MgO–CO_2–H_2O$ system at ambient temperature and atmospheric CO_2 is of essential significance from the standpoint of carbon balance and the removal of green house gases from the atmosphere. A better understanding of the global masses of Mg and CO_2 and the thermal stability of the hydrated carbonates of magnesium will provide a practical understanding for carbon dioxide removal. From a practical point of view, the exact knowledge of the reaction path in $MgO–CO_2–H_2O$ system is of great significance to the performance of brucite and related minerals for green house gas removal. The reaction path involving carbonation of brucite ($Mg(OH)_2$) is particularly complex, as Mg has a strong tendency to form a series of metastable hydrous carbonates. These metastable hydrous carbonates include hydromagnesite ($Mg_5(CO_3)_4(OH)_2·4H_2O$, or $Mg_4(CO_3)_3(OH)_2·3H_2O$), artinite ($Mg_2CO_3(OH)_2·3H_2O$), nesquehonite ($MgCO_3·3H_2O$), and lansfordite ($MgCO_3·5H_2O$). The free energy of formation for these hydroxy and hydrous carbonates differ and their formation depends on the partial pressure of CO_2. In this work we report the synthesis of one of these hydrous carbonate minerals namely hydromagnesite and the thermal stability using dynamic and controlled rate thermal analysis (CRTA) of synthetic hydromagnesite.

Experimental

Synthesis of hydromagnesite

The literature contains a number of methods for the synthesis of single phase nesquehonite and hydromagnesite. Various authors [6, 56–59] have discussed the effects of temperature and partial pressure of carbon dioxide p_{CO_2} on the stability of the synthetic products. A thermal stability study conducted Lanas *et al.* [14] discussed the inherent difficulty associated with studying the $MgO–CaO–H_2O–CO_2$ system as there are multiple complex minerals which can form during the dolomitization process. Synthetic hydromagnesite used in this study were synthesised by the wet chemical method which involved selective precipitation of each mineral by varying the carbonate buffering solution.

It was found that nesquehonite was preferentially precipitated from solution when equimolar amounts of 0.5 M $Mg(NO_3)_2$ and 0.5 M 100% HCO_3^- solutions were mixed drop wise over a period of 10 min at controlled reaction temperature of 45°C. The precipitate was then transferred to a centrifuge to be spun down. At this point it is interesting to note that the precipitate dissolved forming a clear solution. The liquor was left in the centrifuge tube for a week and a new precipitate was found to have formed producing large crystals. It is hypothesised that the initial precipitate was in fact $MgHCO_3$ although subsequent experiments failed to trap the initial precipitate for analysis. Hydromagnesite was synthesised in a similar method to that of nesquehonite only the carbonate solution was replaced with a 0.5 M 100% CO_3^{2-} stock solution. Reaction parameters otherwise were identical to that of the nesquehonite synthesis. The precipitate was centrifuged to separate from the mother liquor and was then washed three times. The synthesised mineral was characterised for phase specificity using XRD, and chemical composition by EDX methods.

Thermal analysis

Dynamic experiment

Thermal decomposition of the hydromagnesite was carried out in a Derivatograph PC type thermoanalytical equipment (Hungarian Optical Works, Budapest, Hungary) capable of recording the thermogravimetric (TG), derivative thermogravimetric (DTG) and differential thermal analysis (DTA) curves simultaneously. The sample was heated in a ceramic crucible in static air atmosphere at a rate of 5°C min^{-1}.

Controlled rate thermal analysis experiment

Thermal decomposition of the hydromagnesite was carried out in a Derivatograph PC type thermoanalytical instrument in a flowing air atmosphere (250 cm^3 min^{-1}) at a pre-set, constant decomposition rate of 0.10 mg min^{-1}. (Below this threshold value the samples were heated under dynamic conditions at a uniform rate of 1.0°C min^{-1}). The samples were heated in an open ceramic crucible at a rate of 0.10°C min^{-1} up to 300°C. With the quasi-isothermal, quasi-isobaric heating program of the instrument the furnace temperature was regulated precisely to provide a uniform rate of decomposition in the main decomposition stage.

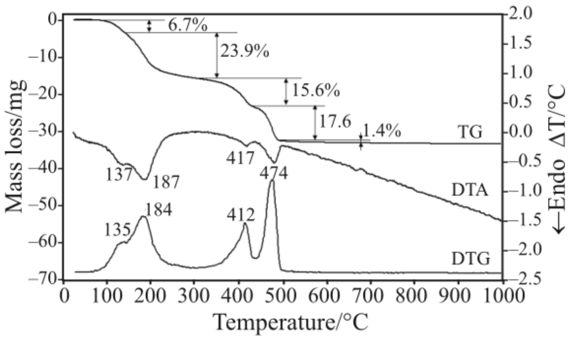

Fig. 1 Dynamic thermal analysis of nesquehonite

Table 1 Decomposition stages under dynamic conditions of hydromagnesite

Decomposition process	Hydromagnesite		
	Temp. range/°C	Mass loss	
		mg	%
Dehydration	24–140	3.4	6.7
Dehydration	140–294	12.2	23.9
Dehydroxylation	294–436	8.0	15.6
Decarbonation	436–498	9.0	17.6
Oxygen loss	498–855	0.7	1.4

Results and discussion

Dynamic thermal analysis of hydromagnesite

The dynamic thermal analysis of hydromagnesite is shown in Fig. 1 where the TG, DTG and DTA patterns are reported. Thermal decomposition in the TG patterns occurs at four temperatures at 135, 184, 412 and 474°C with mass losses of 6.7, 23.9, 15.6 and 17.6%. The results of the dynamic thermal analysis are reported in Table 1. The total mass loss as determined by the TG analysis is 63.8%. The theoretical mass loss based upon the formula above is 60.52%, made up of 37.77% for decarbonation, 15.45% for water loss and 7.30% for OH unit loss. Thus the experimental mass loss is slightly greater than the theoretical mass loss. The first two thermal decomposition steps are attributed to dehydration and dehydroxylation. The last two steps are assigned to decarbonation.

First thermal decomposition step at 135°C:

$$Mg_5[(CO_3)_4(OH)_2]\cdot 4H_2O \rightarrow$$
$$Mg_5[(CO_3)_4(OH)_2]\cdot 2H_2O + 2H_2O$$

Second thermal decomposition step at 184°C:

$$Mg_5[(CO_3)_4(OH)_2]\cdot 2H_2O \rightarrow Mg_5[(CO_3)_4(OH)_2] + 2H_2O$$

Third thermal decomposition step at 412°C:

$$Mg_5[(CO_3)_4(OH)_2] \rightarrow 4MgCO_3 + MgO + H_2O$$

Decarbonation occurs at both 412 and 474°C with 15.6 and 17.6% mass loss according to the reaction:

Fourth thermal decomposition step at 474°C:

$$4MgCO_3 \rightarrow 4MgO + 4CO_2$$

In the DTA patterns endotherms are observed at 137, 187, 417 and 474°C, the values of which correspond to the mass loss steps in the TG curves. These values appear to differ from those reported by Beck [1]. The DTA patterns of hydromagnesite as reported by Beck differ from the results reported here. Beck found the DTA patterns to start slowly at 275°C up to 325°C with the loss of water of crystallisation. The loss of CO_2 was reported to begin at 485 and reached a doublet at 565 and 600°C [1]. The results of Beck are so significantly different that the measurement is open to question. Beck also claims that the product of the reaction is amorphous MgO which changes to a cubic structure through an exothermic step at 510°C. However no exothermic step was observed in our DTA pattern. The difference may be due to the way in which the experiments were conducted.

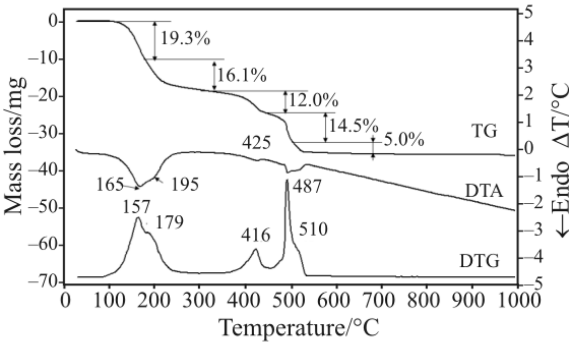

Fig. 2 Dynamic thermal analysis of nesquehonite

It is very interesting to compare the dynamic thermal analysis of nesquehonite with hydromagnesite (Fig. 2). In the DTA patterns for hydromagnesite endotherms are observed at 137, 187, 417 and 474°C. In the DTA patterns for nesquehonite endotherms are observed at 165, 195, 425 and 487°C. The only difference is an additional endotherm at around 510°C. The endotherms occur at very similar temperatures. This observation leads to the conclusion that the mechanism for the decomposition of nesquehonite is very similar to that of hydromagnesite. Davies and Bubelba reported that a synthetic nesquehonite decomposed to hydromagnesite through an intermediate phase which has an XRD pattern of dypingite [60].

Controlled rate thermal analysis of hydromagnesite

The CRTA pattern of hydromagnesite is shown in Fig. 3. Five thermal decomposition steps are observed in the CRTA pattern. The result summary is reported

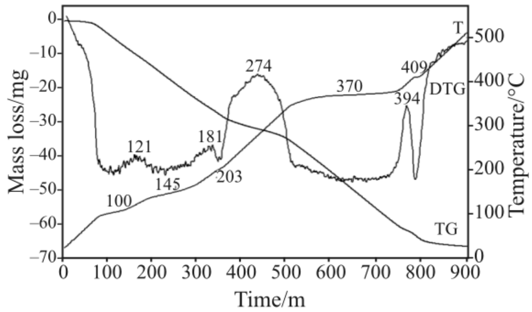

Fig. 3 Dynamic thermal analysis of hydromagnesite

Table 2 Decomposition stages under CRTA conditions of hydromagnesite

Decomposition process	Hydromagnesite/ sample mass: 99.62 mg		
	Temp. range/°C	Mass loss	
		mg	%
Dehydration	25–121	10.0	10.0
Dehydration	121–181	15.1	15.1
Dehydroxylation	181–274	6.8	6.8
Decarbonation	274–394	30.0	30.1
Oxygen loss	394–508	4.8	4.8

in Table 2. There is a quasi-isothermal step at 100°C followed by a second decomposition step at 145°C. As for the dynamic experiment these two steps are attributed to dehydration as is confirmed by ion current curves for gas evolution. A third decomposition step is observed at 203°C. This step is attributed to dehydroxylation. There is along isothermal decomposition step at 370°C which is ascribed to the CO_2 evolution. A second isothermal step at 409°C is observed and the DTG peak is very sharp. One possible assignment of this band is to the MgO recrystallisation from an amorphous to a cubic structure as was suggested by beck in the dynamic DTA experiment. It is noted that the CRTA of nesquehonite (Fig. 4) is very similar to that of hydromagnesite as is the results of the dynamic TG experiment of hydromagnesite and nesquehonite. If a comparison of the data is made, nesquehonite CRTA pattern shows a quasi-isothermal dehydration step at 108 followed by a non-isothermal dehydration step at 145°C and a long time isothermal step at 376°C. Differences may be observed in the CRTA patterns of hydromagnesite and nesquehonite at 203°C attributed to the dehydroxylation of the hydromagnesite and around 409°C.

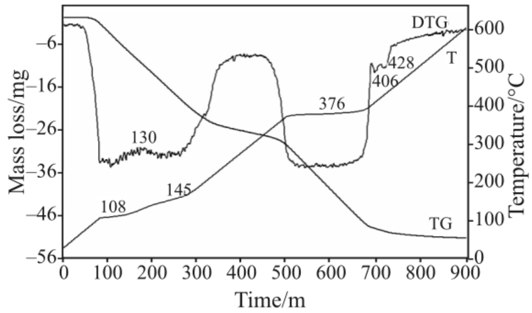

Fig. 4 Controlled rate thermal analysis of hydromagnesite

Conclusions

CRTA technology offers better resolution and a more detailed interpretation of the decomposition processes of magnesium carbonate minerals such as hydromagnesite via approaching equilibrium conditions of decomposition through the elimination of the slow transfer of heat to the sample as a controlling parameter on the process of decomposition. Constant-rate decomposition processes of non-isothermal nature reveal partial collapse of the mineral structure as the hydromagnesite is converted to amorphous MgO, since in this cases a higher energy (higher temperature) is needed to drive out gaseous decomposition products through a decreasing space at a constant, pre-set rate. The CRTA experiment proves the thermal decomposition of hydrated magnesium carbonates from different sources are almost identical. The CRTA technology offers a mechanism for the study of the thermal decomposition of minerals such as hydromagnesite ad nesquehonite.

Appendix

Calculation of water content for hydromagnesite

Composition: $Mg_5(CO_3)_4(OH)_2{\cdot}xH_2O$

Removing water up to 121°C: 10.0 mg that is 0.555 mmol

Remaining dehydrated mineral up to 121°C: 89.62 mg that is 0.227 mmol

Molar mass of dehydrated mineral: 395.61 g mol^{-1}

Calculation of *x*:

1 mol dehydrated mineral – x mol H_2O

0.227 mol dehydrated mineral – 0.555 mol H_2O

x=2.4~2 mol

Formula: $Mg_5(CO_3)_4(OH)_2{\cdot}2H_2O$

Acknowledgements

This research was supported by the Hungarian Scientific Research Fund (OTKA) under grant No. K62175. The financial and infra-structure support of the Queensland University of Technology Inorganic Materials Research Program is gratefully acknowledged.

References

1 C. W. Beck, Am. Mineral., 35 (1950) 985.
2 G. Cocco, Periodico di Mineralogia, 20 (1951) 92.
3 W. E. Ford and W. A. Bradley, Am. J. Sci., 42 (1916) 59.
4 V. P. Ivanova, Zapiski Vserossiiskogo Mineralogicheskogo Obshchestva, 90 (1961) 50.
5 J. L. Jambor, Can. Mineral., 8 (1964) 92.
6 G. Cesaro, Bull. Acad. Roy. Belg., (1910) 844.
7 R. Ballo and L. Jugovics, Földtani Közlöny, 45 (1915) 221; 286.
8 A. E. Mitchell, J. Chem. Soc., Trans., 123 (1923) 1887.
9 G. R. Levi, Annali di Chimica Applicata, 14 (1924) 265.
10 F. L. Cuthbert and R. A. Rowland, Am. Mineral., 32 (1947) 111.
11 W. Zabinski, Rocznik Polsk. Towarz. Geol., 26 (1957) 51.
12 A. Botha and C. A. Strydom, J. Therm. Anal. Cal., 71 (2003) 987.
13 W. B. White, Am. Mineral., 56 (1971) 46.
14 J. Lanas and J. I. Alvarez, Thermochim. Acta, 421 (2004) 123.
15 R. M. Dell and S. W. Weller, Trans. Faraday Soc., 55 (1959) 2203.
16 H. Fan, K. Tao, Y. Xie and K. Wang, Yanshi Xuebao, 19 (2003) 169.
17 W. Hong, S. He, S. Huang, Y. Wang, H. Hou and X. Zhu, Guangpuxue Yu Guangpu Fenxi, 19 (1999) 546.
18 O. S. Pokrovskii, Litologiya i Poleznye Iskopaemye, (1996) 531.
19 F. L. Sayles and W. S. Fyfe, Geochim. Cosmochim. Acta, 37 (1973) 87.
20 S. Iro and J. Sevc, Acta Geologica Universitatis Comenianae, 55 (2000) 73.
21 G. Baron, S. Caillere, R. Lagrange and T. Pobeguin, Bull. Soc. Franc. Mineral. Crist., 82 (1959) 150.
22 A. R. Alderman, Geochim. Cosmochim. Acta, 29 (1965) 1355.
23 E. C. Kirchner nad P. Simonsberger, Karinthin, 87 (1982) 395.
24 R. Brousse, A. Lambert and F. Chantret, Comptes Rendus du Congrès National des Sociétés Savantes, Section des Sciences, 95 (1975) 207.
25 R. Fischbeck and G. Mueller, Contrib. Mineral. Petrol., 33 (1971) 87.
26 V. C. Whitehead, T. C. Keener and S.-J. Khang, 93rd Proceedings of the Air and Waste Management Association's Annual Conference and Exhibition, Salt Lake City, UT, USA, June 18–22, 2000, 5437–5446.
27 S. W. M. Blake and C. Cuff, Preparation and use of cationic halides, sequestration of carbon dioxide. (Perma-Carb Pty Ltd, Australia). Application: WO, 2007, p. 66.
28 J. M. Bouzaid, R. L. Frost, A. W. Musumeci and W. N. Martens, J. Therm. Anal. Cal., 86 (2006) 745.
29 R. L. Frost, J. M. Bouzaid, A. W. Musumeci, J. T. Kloprogge and W. N. Martens, J. Therm. Anal. Cal., 86 (2006) 437.
30 R. L. Frost and Z. Ding, Thermochim. Acta, 397 (2003) 119.
31 R. L. Frost and Z. Ding, Thermochim. Acta, 405 (2003) 207.
32 R. L. Frost, Z. Ding and H. D. Ruan, J. Therm. Anal. Cal., 71 (2003) 783.
33 R. L. Frost, K. L. Erickson, M. L. Weier, A. R. McKinnon, P. A. Williams and P. Leverett, Thermochim. Acta, 427 (2005) 167.
34 R. L. Frost, J. Kristóf, W. N. Martens, M. L. Weier and E. Horváth, J. Therm. Anal. Cal., 83 (2006) 675.
35 R. L. Frost, W. Martens and M. O. Adebajo, J. Therm. Anal. Cal., 81 (2005) 351.
36 R. L. Frost, D. L. Wain, R.-A. Wills, A. Musemeci and W. Martens, Thermochim. Acta, 443 (2006) 56.
37 R. L. Frost and M. L. Weier, Thermochim. Acta, 409 (2004) 79.
38 R. L. Frost and M. L. Weier, Thermochim. Acta, 406 (2003) 221.
39 R. L. Frost, M. L. Weier and W. Martens, J. Therm. Anal. Cal., 82 (2005) 373.
40 R. L. Frost, R. -A. Wills, J. T. Kloprogge and W. Martens, J. Therm. Anal. Cal., 84 (2006) 489.
41 R. L. Frost, R. -A. Wills, J. T. Kloprogge and W. N. Martens, J. Therm. Anal. Cal., 83 (2006) 213.
42 R. L. Frost and K. L. Erickson, J. Therm. Anal. Cal., 76 (2004) 217.
43 R. L. Frost, K. Erickson and M. Weier, J. Therm. Anal. Cal., 77 (2004) 851.
44 R. L. Frost, M. L. Weier and K. L. Erickson, J. Therm. Anal. Cal., 76 (2004) 1025.
45 R. L. Frost and M. L. Weier, J. Therm. Anal. Cal., 75 (2004) 277.
46 R. L. Frost, W. Martens, Z. Ding and J. T. Kloprogge, J. Therm. Anal. Cal., 71 (2003) 429.
47 R. L. Frost, S. J. Palmer, J. M. Bouzaid and B. J. Reddy, J. Raman Spectrosc., 38 (2007) 68.
48 R. L. Frost, D. A. Henry, M. L. Weier and W. Martens, J. Raman Spectrosc., 37 (2006) 722.
49 R. L. Frost, A. W. Musumeci, J. T. Kloprogge, M. O. Adebajo and W. N. Martens, J. Raman Spectrosc., 37 (2006) 733.
50 R. L. Frost, J. Cejka, M. Weier and W. N. Martens, J. Raman Spectrosc., 37 (2006) 879.
51 R. L. Frost, M. L. Weier, J. Cejka and J. T. Kloprogge, J. Raman Spectrosc., 37 (2006) 585.
52 R. L. Frost, J. Cejka, M. L. Weier and W. Martens, J. Raman Spectrosc., 37 (2006) 538.
53 R. L. Frost, M. L. Weier, B. J. Reddy and J. Cejka, J. Raman Spectrosc., 37 (2006) 816.
54 R. L. Frost, M. L. Weier, W. N. Martens, J. T. Kloprogge and J. Kristóf, J. Raman Spectrosc., 36 (2005) 797.
55 R. L. Frost, R.-A. Wills, M. L. Weier and W. Martens, J. Raman Spectrosc., 36 (2005) 435.
56 Magnesium carbonate in the form of nesquehonite or lansfordite. (Basic Refractories Inc.). G, 1946.
57 G. Cesaro, Bull. Sci. Acad. Roy. Belg., (1910) 749.
58 E. D. Glover and R. F. Sippel, Geochim. Cosmochim. Acta, 31 (1967) 603.
59 B. Valuziene, A. Kaminskas and K. Gasiunas, Sb. Tr. VNII Teploizolyats. i Akust. Stroit. Materialov i Izdelii, (1976) 183.
60 P. J. Davies and B. Bubela, Chem. Geology, 12 (1973) 289.

Received: October 24, 2007
Accepted: November 19, 2007

DOI: 10.1007/s10973-007-8845-6